

# **The decreasing albedo of the Zhadang glacier on western Nyainqentanglha and the role of light-absorbing impurities**

B. Qu<sup>4,1</sup>, J. Ming<sup>1,2,3</sup>, S.-C. Kang<sup>1,4</sup>, G.-S. Zhang<sup>4</sup>, Y.-W. Li<sup>4</sup>, C.-D. Li<sup>4</sup>, S.-Y. Zhao<sup>5</sup>, Z.-M. Ji<sup>4</sup>, and J.-J Cao<sup>5</sup>

1 State Key Laboratory of Cryospheric Sciences, Cold and Arid Regions Environmental and Engineering Research Institute, Chinese Academy of Sciences, Lanzhou, China

2 Collaborative Innovation Centre on Forecast and Evaluation of Meteorological Disasters, Nanjing University of Information Science & Technology, Nanjing, China

3 National Climate Centre, China Meteorological Administration (CMA), Beijing, China

4 Key Laboratory of Tibetan Environment Changes and Land surface Processes, Institute of Tibetan Plateau Research, Chinese Academy of Sciences, Beijing, China

5 State Key Laboratory of Loess and Quaternary Geology, Institute of Earth Environment, Chinese Academy of Sciences, Xi'an, China

Corresponding author: J. Ming (petermingjing@hotmail.com)

## Abstract

A large change in albedo has a significant effect on glacier ablation. Atmospheric aerosols (e.g., black carbon (BC) and dust) can reduce the albedo of glaciers and thus contribute to their melting. In this study, we investigated the measured albedo as well as the relationship between the albedo and the mass balance in Zhadang glacier on Mt. Nyainqentanglha associated with MODIS (10A1) data. The impacts of BC and dust in albedo reduction in different melting conditions were identified with the SNow ICe Aerosol Radiative (SNICAR) model and in-situ data. The mass balance of the glacier has a significant correlation with its surface albedo derived from the Moderate Resolution Imaging Spectroradiometer (MODIS) on-board the Terra satellite. The average albedo of the Zhadang glacier from the MODIS increased with the altitude and fluctuated but had a decreasing trend during the period 2001–2012, with the highest (0.722) in 2003 and the lowest (0.597) in 2009 and 2010. Snow samples were collected to measure the BC and dust in the Zhadang glacier in the summer of 2012. The sensitivity analysis via SNICAR showed that BC was a major factor in albedo reduction when the glacier was covered by newly fallen snow. Nevertheless, the contribution of dust to albedo reduction can be as high as 58% when the glacier experiences strong surficial melting where the surface was almost bare ice. The average radiative forcing (RF) caused by dust could increase from 1.1 to 8.6 W m<sup>-2</sup>, exceeding the forcings caused by BC after snow was deposited and surface melting occurred in the Zhadang glacier. This suggests that it may be dust rather than BC that dominates the melting of some glaciers in the TP during melting seasons.

## 1. Introduction

1 Glaciers and snow cover are important reservoirs of fresh water on Earth. A rough volume of  
2  $2.4 \times 10^7$  km<sup>3</sup> of water is stored in them (Oki and Kanae, 2006), and changes in these  
3 reservoirs have a significant effect on the water supply in many regions of the world (Mote et  
4 al., 2003; Yao et al., 2012). The Tibetan Plateau (TP) is the source of many great rivers (e.g.,  
5 Yangtze, Yellow, Indus, Ganges, and Brahmaputra rivers), which concentrate their sources at  
6 the glaciers in the TP known as the “Asian Water Towers”. More than 1.4 billion people  
7 depend on the water from these rivers (Immerzeel et al., 2010), but these glaciers have been  
8 undergoing rapid changes (Kang et al., 2010; Yao et al., 2012). Therefore, it is important to  
9 understand the impact factors that affect the glaciers and snow cover.

10

11 The surface energy budget of glaciers has significant effects on their ablation (Zhang et al.,  
12 2013), and snow/ice albedo is one of the most important parameters that affect the absorbed  
13 radiation. Snow/ice albedo is defined as the fraction of the reflected and the incident radiant  
14 flux in the surface of the snow/ice. A higher albedo implies a cleaner snow surface or less  
15 energy available for melting. Clean snow has the highest albedo (as high as 0.9) of any natural  
16 substance, but this diminishes when the snow surface is dirty or darkened **due to snow grain**  
17 **size increases** (Warren and Wiscombe, 1980; Wiscombe and Warren, 1980). A recent report  
18 (Lhermitte et al., 2012) indicates a darkening surface of the Greenland ice sheet and a rapidly  
19 decreasing albedo during 2000–2011, which will greatly increase the rate of mass loss of the  
20 ice sheet as more solar energy is absorbed by the darker glacial ice (Farmer and Cook, 2013).

21

22 Temperature, precipitation, and glacial dynamic processes are the key factors that affect  
23 glacial change (Sugden and John, 1976). However, there is now a general consensus that  
24 light-absorbing constituents (LACs, e.g., BC and dust) can reduce the albedo of glaciers  
25 (dirtying or darkening effect) and thus also contribute to the mass loss of glaciers. Both BC  
26 and dust are important absorbers of solar radiation in the visible spectrum (Warren and  
27 Wiscombe, 1980; Hadley and Kirchstetter, 2012; IPCC, 2007), and BC has an absorbing  
28 capacity approximately 50 to 200 times greater than dust (Warren and Wiscombe, 1980). The  
29 impacts of BC and dust deposited on the TP glaciers (in particular, on their radiation balance)

30 have been reported in previous literature (Ming et al., 2009a, 2013a). Simulation of the effect  
31 of LACs on the albedo of Himalayan glaciers showed that LACs in this region had a  
32 contribution of 34% to the albedo reduction during the late spring time, with 21% due to BC  
33 and 13% originating from dust (Ming et al., 2012).

34

35 The lowering of the surface albedo due to the presence of a dust layer could also lead to a  
36 drastic increase in the glacier melting rate during the melting season (Fujita, 2007). In general,  
37 BC can be transported over long distances (Ming et al., 2010), whereas dust usually comes  
38 from the local or regional environment of the glaciers (Kang et al., 2000). Historical  
39 deposition records of BC revealed by ice cores and lake sediments over the TP indicate that  
40 BC originating from south and central Asia has reached the glaciers in recent decades (Ming  
41 et al., 2008; Xu et al., 2009b; Cong et al., 2013).

42

43 There has been extensive research focusing on quantifying the impact of LACs in ice cores  
44 and snow cover to understand the relationship between LACs and albedo reduction (Aoki et  
45 al., 2011; Painter et al., 2007, 2012; Ginot et al., 2013; Kaspari et al., 2013). However, few  
46 researchers discussed the exact effects that BC and dust have on different types of glacier  
47 surfaces during the melting season. Dust sometimes causes significant spatial variation of the  
48 surface albedo in glaciers. Moreover, glacier melting causes LAC particles to concentrate in  
49 the surface and to further enhance the absorption of radiation. This positive feedback  
50 highlights the importance of investigating LACs and their effects on the albedo and glacial  
51 melt across a whole glacier, particularly in the prevailing situation where glaciers are  
52 shrinking and emissions of BC are increasing (Bond et al., 2013). In this work, we investigate  
53 the spatial distribution of LACs from the terminate along to the accumulation zone of the  
54 Zhadang glacier, southern TP during the summer of 2012 and estimate the contribution of BC  
55 and dust to the albedo reduction in different melting conditions.

56

## 57 **2. Methodology**

58 The Zhadang glacier is located in western Nyainqentanglha, southern TP, (30°28.57'N,  
59 90°38.71'E, and 5500-5800 m a.s.l.) (Fig. 1). Surface snow/ice samples were collected, and  
60 the surface albedo was observed on Zhadang glacier during 12-16 July and 24-27 August,

61 2012.

62

63 We classified three conditions or scenarios of the glacier surface: (1) S-I: the surface of the  
64 glacier is bare ice containing some visible dark constituents (Fig. 2a); (2) S-II: the surface is  
65 covered by aged snow/firn (Fig. 2a); (3) S-III: the surface is covered by fresh snow (Fig. 2b).  
66 These surface conditions are typical in most alpine glaciers throughout the year (Benn and  
67 Evans, 2010). A description of the sampling details in the Zhadang glacier is given in Table 1.  
68

## 69 **2.1 Albedo data from the Moderate Resolution Imaging Spectroradiometer** 70 **(MODIS) on-board Terra**

71 The MODIS albedo data were used to investigate the albedo change in the Zhadang glacier.  
72 The series of the product is the MODIS/Terra Snow Cover Daily L3 Global 500m Grid  
73 (MOD10A1), which is based on a snow mapping algorithm that employs a normalised  
74 difference snow index (NDSI) and other criteria tests (Riggs and Hall, 2011). The MOD10A1  
75 product contains four data layers: snow cover, snow albedo, fractional snow cover, and **binary**  
76 quality assessment (QA), which is **assigned as “good” or “bad”**. The data are compressed in  
77 hierarchical data format-Earth observing system (HDF-EOS) and are formatted along with the  
78 corresponding metadata. The images of MOD10A1 are 1200 km by 1200 km tiles with a  
79 resolution of 500 m × 500 m gridded in a sinusoidal map projection. Data are available from  
80 24 February 2000 to present via FTP (Hall et al., 2006). The snow albedo data used in the  
81 calculation are based on three **expected** criteria: the pixels are identified as snow cover,  
82 fractional snow cover is 100, and the pixels pass the QA. The MODIS daily albedo has high  
83 accuracy in flat terrain (Stroeve et al., 2006; Tekeli et al., 2006.), but it shows some errors in  
84 complex topography, such as mountainous regions (Sorman et al., 2007; Warren, 2013).

85

86 To verify the applicability of the MOD10A1 product in the Zhadang glacier, we used the  
87 observed data measured by the Kipp & Zonen radiometers mounted on an automatic weather  
88 station (AWS) that was set in the saddle of the glacier (5680 m a.s.l., Fig. 1). The albedo data  
89 were extracted from the precise pixel in the relevant MODIS image where the AWS was  
90 located. The observed albedos were selected in the local time period of 12:30 to 13:30 LT,  
91 considering the scanning time of the Terra satellite passing over the study area. The  
92 correlation analysis between the MODIS data and the observed data showed a good

93 relationship at the confidence level of 0.02 (Fig. 3), indicating that it is reasonable to use  
94 MOD10A1 data to study the albedo change of the Zhadang glacier.

95

## 96 **2.2 Field albedo observation**

97 Warren (2013) suggested that it is unlikely to detect the impact of black carbon on snow  
98 albedo by remote sensing. In this work, a spectroradiometer (Model ASD<sup>®</sup> FS-3) was used to  
99 measure the spectral albedo of the glacier. This covers a radiation waveband of 350-2500 nm  
100 with a wavelength resolution of one nanometre. The optical sensor of the spectroradiometer  
101 was set in a pistol-shape device so that the optical fibre can be fixed inside and mounted on  
102 the rocker arm of the tripod with a gradienter for levelling. The distance between the sensor  
103 and the snow surface was approximately 0.5 m, allowing for the measurement of the spectral  
104 reflectances. Air temperature has been recorded by an autonomous weather station (AWS)  
105 built up in the accumulative zone of the Zhadang glacier since 2008 (Fig. 1).

106

107 During the expedition of July 2012, we measured the surface albedo and collected snow  
108 samples in S-I (two sites: A and B) and S-II (C and D) conditions. In August, the glacier was  
109 covered by newly fallen snow, and the albedo and surface snow samples were successfully  
110 observed and collected at eight sites in S-III conditions (Fig. 2). Along with the sampling,  
111 other necessary parameters, such as snow density, and grain sizes, for simulating the surface  
112 albedo were also observed. Details concerning the simulations of the surface albedo have  
113 been introduced in a previous work (Ming et al., 2013a).

114

## 115 **2.3 Snow/ice sampling and BC/dust measurement**

116 Snow/ice samples were collected in accordance with the “Clean Hands-Dirty Hands”  
117 principle, meaning that the person whose hands are collecting sampling will not touch any  
118 other material that may contaminate the snow samples (Fitzgerald, 1999). We collected two  
119 parallel samples 10 cm away from each other from the surface to 5 cm depth at each site when  
120 measuring the albedo. The snow density was measured using a balance. The samples were  
121 stored in NALGENE<sup>®</sup> HDPE wide-mouth bottles (250 mL) and were kept frozen until  
122 laboratory analysis. The snow grain sizes were measured using a hand lens (25X) with an

123 accuracy of 0.02 mm; the largest length of a single ice crystal was also measured using a  
124 snow crystal card with 1 mm grids (Aoki et al., 2007). We filtered the snow melt water  
125 through quartz-fibre filters, which were weighed before and after the filtration using a  
126 microbalance to evaluate the mass of on-load dust. A thermal-optical method of carbon  
127 analysis, using DRI<sup>®</sup> Model 2001A OC/EC (Chow et al., 1993), was employed to measure the  
128 BC mass in the samples.

129

## 130 **2.4 Albedo reduction modelling and radiative forcing (RF)**

131 The Snow-Ice-Aerosol-Radiative (SNICAR) model can be used to simulate the hemisphere  
132 albedo of snow and ice for unique combinations of impurity contents (BC, dust, and volcanic  
133 ash), snow **grain** size, and incident solar flux characteristics (Flanner et al., 2007). It was  
134 applied to simulate the albedo variation caused by BC and dust deposited in the glacier  
135 surface in this work. We conducted a series of sensitivity analyses to identify the impact of  
136 BC and dust on albedo reduction in three different surface conditions of the Zhadang glacier  
137 (also see Section 2.2). The solar zenith angle was identified based on the time and position of  
138 the specific sampling sites. The snow grain effective radius is taken as half the observed snow  
139 grain size **introduced by Aoki et al. (2007)** and is shown in Table 1. The albedo of the  
140 underlying **bare ice** is taken as 0.11-0.19 in the visible band and 0.18-0.23 in the near-infrared  
141 band **as measured in-situ by the spectroradiometer. We use the default value 1 as the mass**  
142 **absorption cross section (MAC) scaling factor (experimental) in the modelling.** The detailed  
143 parameters used in SNICAR are listed in the appendix.

144 RF was defined using the equation below,

$$145 \quad RF = R_{in-short} * \Delta\alpha,$$

146 where  $R_{in-short}$  denotes the incident solar radiation measured by radiometer, and  $\Delta\alpha$  denotes the  
147 reduction of the albedo.

148

## 149 **3. Results and Discussion**

### 150 **3.1 Surface albedo variations of the Zhadang glacier into the 21<sup>st</sup> century**

151 The albedo of the Zhadang glacier increased with elevation (Table 1) due to the lower

152 temperature favouring more cold snow stored in higher elevations. The MODIS albedo of the  
153 Zhadang glacier shows an obvious decreasing trend of  $0.003 \text{ a}^{-1}$  during the period 2001 –  
154 2012, despite the inter-annual fluctuations (Fig. 4). The annual average albedo declined from  
155 0.676 in 2001 to 0.597 in 2010 with a maximum of 0.722 in 2003 and a minimum of 0.597 in  
156 2009 and 2010. This trend was also revealed in the Himalayan and Tanggula glaciers (Ming et  
157 al., 2012; Wang et al., 2012). Regional air temperature shows a decreasing trend during the  
158 period 2008-2012, which seemed not to contribute the decreasing albedo (Fig. 4).

159  
160 The surface albedo of a specific glacier could be linked with its mass balance in the TP, which  
161 has been proved by Wang et al. (2013). We used the observed mass balance data from 2006  
162 through 2010 in the Zhadang glacier (Zhang et al., 2013) to perform a correlation analysis  
163 with the glacier surface albedo (Fig. 4). A lower albedo is related to larger negative balances  
164 and vice versa. For example, the most negative mass balance of the Zhadang glacier appeared  
165 in 2010 when the albedo of the glacier reaches the minimum, whereas the most positive mass  
166 balance occurred in 2008, and the albedo was the highest during the period 2006-2010. The  
167 significant positive correlation ( $n = 7, \alpha = 0.01, R^2 > 0.83$ ) between the albedo and the mass  
168 balance of the glacier indicates that the surface albedo of the Zhadang glacier is a strong index  
169 of the glacier mass balance.

### 170 171 **3.2 Impacts of BC and dust on the albedo**

172 The impacts of BC and dust concentrations, as well as other observations, such as snow grain  
173 size, snowpack density, and snowpack thickness, on the Zhadang glacier are shown in Table 1.  
174 In S-I conditions, the concentration of dust varied from 504–1892 ppm with an average of  
175 1198 ppm, whereas BC was 334–473 ppb with an average of 404 ppb. In S-II conditions, the  
176 concentrations of BC and dust ranged from 81 to 143 ppb with an average of 112 ppb and  
177 from 34 to 67 ppm with an average of 50 ppm, respectively. However, the concentration of  
178 BC in S-III was 41 to 59 ppb with an average of 52 ppb, whereas the dust concentration was 3  
179 to 8 ppm with an average of 6 ppm.

180  
181 There are large differences in the BC and dust concentrations in the surface of the Zhadang  
182 glacier in different scenarios of surface features (Fig. 2a). In S-I and S-II, intensive surface  
183 melting could lead to a strong enrichment of LACs in the surface of the glacier. In S-III



184 conditions, the Zhadang glacier was covered by fresh snow due to frequent snowfalls at night  
185 (Fig. 2b). Thus, the concentrations of LACs in S-III are several magnitudes lower than those  
186 in S-I and S-II conditions (Table 1). Table 2 provides observed and simulated albedos at the  
187 sampling sites. The observed surface albedo increases roughly along with the elevation on the  
188 Zhadang glacier, in contrast with the concentrations of BC and dust in S-I and S-II conditions.  
189 **The correlations of in-situ observed albedo and the albedo simulated by SNICAR after adding**  
190 **measured BC and dust into the snow surface are 0.9992 for S-I, 0.9995 for S-II, and 0.4729**  
191 **for S-III, respectively.** This suggests that the enrichment of BC and dust on the surface of the  
192 glacier could reduce the glacier albedo, thus resulting in the melting of glaciers.

193

194 The sensitivity analysis of the respective impacts of BC and dust on reducing the snow albedo  
195 of the Zhadang glacier was calculated by SNICAR and is shown in Fig. 5. **We assume that the**  
196 **model also works well for thin snow (< 5 cm) with ice beneath. This configuration with the**  
197 **SNICAR model implies that impurities contained within the ice beneath the snow do not**  
198 **contribute to the radiative forcing calculations. It is unclear how important this assumption is,**  
199 **but it may contribute to a low bias in the RF estimates.** We presume three impacting factors  
200 dominating the albedo varying in the glacial surface, i.e., BC, dust, and the grain size growing  
201 due to warming (Ming et al., 2012). Dust exceeding BC was the most dominant factor in  
202 reducing glacier albedo in S-I. BC other than dust dominates albedo reduction in cases where  
203 the glacier was covered by snow (S-II and S-III). The incoming solar irradiances at every  
204 sampling time during the two trips are listed in Table 2.

205

206 We calculated the RF of both BC and dust on the Zhadang glacier. The simulation shows that  
207 the RF caused by BC and dust deposition on the Zhadang glacier varied between 0.4–11.8 W  
208  $\text{m}^{-2}$  and 0.5–16.4 W  $\text{m}^{-2}$ , respectively (Fig. 5). The RF of dust is much higher than that of BC  
209 in S-I, whereas the RF of BC exceeds dust in S-II and S-III. On average, the forcing caused  
210 by dust deposition on the Zhadang glacier in the summer of 2012 was  $2.7 \pm 3.4$  W  $\text{m}^{-2}$ , and  
211 that caused by BC was  $4.8 \pm 3.2$  W  $\text{m}^{-2}$ , which is a lower than that recorded in the northern TP  
212 (Ming et al., 2013b) and higher than recorded in the Arctic (Flanner, 2013; Dou et al., 2012).

213

#### 214 **4. Summary and Conclusions**

215 The albedo of the Zhadang glacier declined throughout the 10 years from 2001–2010,  
216 according to the MODIS data, and had a significant correlation with the mass balance, which  
217 means that remotely sensed albedo data can be used in the research of the mass balance  
218 change of glaciers on a large spatial scale. During the summer of 2012, the average  
219 concentrations of BC and dust were 404 and 1198 ppm on the surface of the Zhadang glacier,  
220 which are one and three magnitudes higher than the 52 ppb of BC and the 6.4 ppm of dust in  
221 fresh snow. The effects of BC and dust on the glacier albedo were quantified based both on  
222 observed and simulated data. The contribution of dust and BC to albedo reduction was 58 and  
223 27%, respectively, when the glacier was covered by bare ice. In the surface covered by aged  
224 snow, 36% of the surface albedo reduction was caused by BC, and 29% was caused by dust.  
225 When the glacier was covered by fresh snow, BC and dust contributed 12 and 3% to albedo  
226 reduction, respectively. BC was a major factor in albedo reduction when the glacier was  
227 covered by fresh and aged snow. Dust made the most significant contribution to albedo  
228 reduction when the glacier was bare-ice covered.

229

#### 230 **Acknowledgements**

231 This work was supported by the Global Change Research Program of China (2010CB951401),  
232 the National Natural Science Foundation of China (Grants 41121001, 41225002, and  
233 41190081), the State Key Laboratory of Cryospheric Sciences, CAS (no. SKLCS-ZZ-  
234 2012-01-06), CMA (no. GYHY201106023), the National Science & Technology Pillar  
235 Program during the Twelfth Five-year Plan Period (2012BAC20B05), and the Climate  
236 Change Science Foundation of CMA (2013-2014). The authors would like to thank H. Zhang  
237 for his great help with processing the albedo data.

238

#### 239 **References**

240 Aoki, T., Hori, M., Motoyoshi, H., Tanikawa, T., Hachikubo, A., Sugiura, K., Yasunari, T. J.,  
241 Storvold, R., Eide, H. A., and Stamnes, K.: ADEOS-II/GLI snow/ice products—Part II:  
242 Validation results using GLI and MODIS data, *Remote Sensing of Environment*, 111, 274-290,  
243 10.1016/j.rse.2007.02.035, 2007.  
244 Aoki, T., Kuchiki, K., Niwano, M., Kodama, Y., Hosaka, M., and Tanaka, T.: Physically based  
245 snow albedo model for calculating broadband albedos and the solar heating profile in

246 snowpack for general circulation models, *Journal of Geophysical Research: Atmospheres*  
247 (1984–2012), 116, 2011.

248 Benn, D. I., and Evans, D. J.: *Glaciers and glaciation*, Hodder Education, 2010.

249 Bond, T., Doherty, S., Fahey, D., Forster, P., Berntsen, T., DeAngelo, B., Flanner, M., Ghan, S.,  
250 Kärcher, B., and Koch, D.: Bounding the role of black carbon in the climate system: A  
251 scientific assessment, *Journal of Geophysical Research: Atmospheres*, 10.1002/jgrd.50171,  
252 2013.

253 Chow, J. C., Watson, J. G., Pritchett, L. C., Pierson, W. R., Frazier, C. A., and Purcell, R. G.:  
254 The DRI thermal/optical reflectance carbon analysis system: description, evaluation and  
255 applications in US air quality studies, *Atmospheric Environment. Part A. General Topics*, 27,  
256 1185-1201, 1993.

257 Cong, Z., Kang, S., Gao, S., Zhang, Y., Li, Q., and Kawamura, K.: Historical trends of  
258 atmospheric black carbon on Tibetan Plateau as reconstructed from a 150-year lake sediment  
259 record, *Environmental science & technology*, 2013.

260 Dou, T., Xiao, C., Shindell, D., Liu, J., Eleftheriadis, K., Ming, J., and Qin, D.: The  
261 distribution of snow black carbon observed in the Arctic and compared to the GISS-PUCCINI  
262 model, *Atmospheric Chemistry and Physics*, 12, 7995-8007, 2012.

263 Farmer, G. T., and Cook, J.: Earth's Albedo, Radiative Forcing and Climate Change, in:  
264 *Climate Change Science: A Modern Synthesis*, Springer, 217-229, 2013.

265 Fitzgerald, W. F.: Clean hands, dirty hands: Clair Patterson and the aquatic biogeochemistry  
266 of mercury, *Clean Hands, Clair Patterson's Crusade Against Environmental Lead*  
267 *Contamination*, 119-137, 1999.

268 Flanner, M. G., Zender, C. S., Randerson, J. T., and Rasch, P. J.: Present-day climate forcing  
269 and response from black carbon in snow, *J. Geophys. Res.*, 112, D11202,  
270 10.1029/2006JD008003, 2007.

271 Flanner, M. G.: Arctic climate sensitivity to local black carbon, *Journal of Geophysical*  
272 *Research: Atmospheres*, 10.1002/jgrd.50176, 2013.

273 Fujita, K.: Effect of dust event timing on glacier runoff: sensitivity analysis for a Tibetan  
274 glacier, *Hydrological Processes*, 21, 2892-2896, 2007.

275 Ginot, P., Dumont, M., Lim, S., Patris, N., Taupin, J., Wagnon, P., Gilbert, A., Arnaud, Y.,  
276 Marinoni, A., and Bonasoni, P.: A 10 yr record of black carbon and dust from Mera Peak ice  
277 core (Nepal): variability and potential impact on Himalayan glacier melting, *Cryosphere*  
278 *Discussions*, 7, 2013.

279 Hall, Dorothy K., George A. Riggs, and Vincent V. Salomonson. MODIS/Terra Snow Cover  
280 Daily L3 Global 500m Grid V005, [January 2001 to December 2010]. Boulder, Colorado  
281 USA: National Snow and Ice Data Centre. Digital media (updated daily), 2006  
282 Immerzeel, W. W., van Beek, L. P., and Bierkens, M. F.: Climate change will affect the Asian  
283 water towers, *Science*, 328, 1382-1385, 2010.  
284 IPCC, C. C.: The Physical Science Basis. Contribution of Working Group I to the Fourth  
285 Assessment Report of the Intergovernmental Panel on Climate Change, Cambridge University  
286 Press, Cambridge, United Kingdom and New York, NY, USA, 996, 2007, 2007.  
287 Kang, S., Wake, C. P., Dahe, Q., Mayewski, P. A., and Tandong, Y.: Monsoon and dust signals  
288 recorded in Dasuopu glacier, Tibetan Plateau, *Journal of Glaciology*, 46, 222-226, 2000.  
289 Kang, S., Xu, Y., You, Q., Flügel, W. A., Pepin, N., and Yao, T.: Review of climate and  
290 cryospheric change in the Tibetan Plateau, *Environmental Research Letters*, 5, 015101, 2010.  
291 Kaspari, S., Painter, T., Gysel, M., and Schwikowski, M.: Seasonal and elevational variations  
292 of black carbon and dust in snow and ice in the Solu-Khumbu, Nepal and estimated radiative  
293 forcings, *Atmospheric Chemistry and Physics Discussions*, 13, 33491-33521, 2013.  
294 Lhermitte, S., Greuell, W., van Meijgaard, E., van Oss, R., van den Broeke, M., and van de  
295 Berg, W.: Greenland ice sheet surface albedo: trends in surface properties (2000-2011), EGU  
296 General Assembly Conference Abstracts, 2012, 12349,  
297 Ming, J., Cachier, H., Xiao, C., Qin, D., Kang, S., Hou, S., and Xu, J.: Black carbon record  
298 based on a shallow Himalayan ice core and its climatic implications, *Atmospheric Chemistry  
299 and Physics*, 8, 1352, 2008.  
300 Ming, J., Xiao, C., Du, Z., and Flanner, M. G.: Black Carbon in snow/ice of west China and  
301 its radiative forcing, *Advances in Climate Change Research*, 92, 114-123, 2009a.  
302 Ming, J., Xiao, C. D., Cachier, H., Qin, D. H., Qin, X., Li, Z. Q., and Pu, J. C.: Black Carbon  
303 (BC) in the snow of glaciers in west China and its potential effects on albedos, *Atmospheric  
304 Research*, 92, 114-123, 2009b.  
305 Ming, J., Xiao, C., Sun, J., Kang, S., and Bonasoni, P.: Carbonaceous particles in the  
306 atmosphere and precipitation of the Nam Co region, central Tibet, *Journal of Environmental  
307 Sciences*, 22, 1748-1756, 2010.  
308 Ming, J., Du, Z., Xiao, C., Xu, X., and Zhang, D.: Darkening of the mid-Himalaya glaciers  
309 since 2000 and the potential causes, *Environmental Research Letters*, 7, 014021, 2012.  
310 Ming, J., Wang, P., Zhao, S., and Chen, P.: Disturbance of light-absorbing aerosols on the  
311 albedo in a winter snowpack of Central Tibet, *Journal of Environmental Sciences*, 337, 2013a.

312 Ming, J., Xiao, C., Du, Z., and Yang, X.: An Overview of Black Carbon Deposition in High  
313 Asia Glaciers and its Impacts on Radiation Balance, *Advances in Water Resources*, 80-87,  
314 2013b.

315 Mote, P. W., Parson, E. A., Hamlet, A. F., Keeton, W. S., Lettenmaier, D., Mantua, N., Miles,  
316 E. L., Peterson, D. W., Peterson, D. L., and Slaughter, R.: Preparing for climatic change: the  
317 water, salmon, and forests of the Pacific Northwest, *Climatic Change*, 61, 45-88, 2003.

318 Oki, T., and Kanae, S.: Global hydrological cycles and world water resources, *science*, 313,  
319 1068-1072, 2006.

320 Painter, T. H., Barrett, A. P., Landry, C. C., Neff, J. C., Cassidy, M. P., Lawrence, C. R.,  
321 McBride, K. E., and Farmer, G. L.: Impact of disturbed desert soils on duration of mountain  
322 snow cover, *Geophysical Research Letters*, 34, 2007.

323 Painter, T. H., Skiles, S. M., Deems, J. S., Bryant, A. C., and Landry, C. C.: Dust radiative  
324 forcing in snow of the Upper Colorado River Basin: 1. A 6 year record of energy balance,  
325 radiation, and dust concentrations, *Water Resources Research*, 48, 2012.

326 Riggs G, Hall D: MODIS snow and ice products, and their assessment and applications, *Land*  
327 *Remote Sensing and Global Environmental Change*. Springer New York, 681-707, 2011.

328 Sorman, A., Akyürek, Z., Sensoy, A., Sorman, A., and Tekeli, A.: Commentary on comparison  
329 of MODIS snow cover and albedo products with ground observations over the mountainous  
330 terrain of Turkey, *Hydrol. Earth Syst. Sci*, 11, 1353-1360, 2007.

331 Stroeve, J. C., Box, J. E., and Haran, T.: Evaluation of the MODIS (MOD10A1) daily snow  
332 albedo product over the Greenland ice sheet, *Remote Sensing of Environment*, 105, 155-171,  
333 2006.

334 Sugden, D. E., and John, B. S.: *Glaciers and landscape: a geomorphological approach*,  
335 Edward Arnold London, 1976.

336 Tekeli, A. E., Şensoy, A., Şorman, A., Akyürek, Z., and Şorman, Ü.: Accuracy assessment of  
337 MODIS daily snow albedo retrievals with in situ measurements in Karasu basin, Turkey,  
338 *Hydrological processes*, 20, 705-721, 2006.

339 Wang, J., B. Ye, Y. Cui, X. He, and G. Yang: Spatial and temporal variations of albedo on nine  
340 glaciers in western China from 2000 to 2011, *Hydrol Process.*, doi:10.1002/hyp.9883, 2013

341 Wang, Q., Jacob, D., Fisher, J., Mao, J., Leibensperger, E., Carouge, C., Sager, P., Kondo, Y.,  
342 Jimenez, J., and Cubison, M.: Sources of carbonaceous aerosols and deposited black carbon in  
343 the Arctic in winter-spring: implications for radiative forcing, *Atmospheric Chemistry and*  
344 *Physics*, 11, 12453-12473, 2011.

345 Warren, S.G., Wiscombe, W.J. A model for the spectral albedo of snow. II: Snow containing  
346 atmospheric aerosols. *J. Atmos. Sci* 37, 2734-2745, 1980.

347 Warren, S. G.: Can black carbon in snow be detected by remote sensing?, *Journal of*  
348 *Geophysical Research: Atmospheres*, 118, 779-786, 2013.

349 Wiscombe, W.J., Warren, S.G. A model for the spectral albedo of snow. I: Pure snow. *Journal*  
350 *of the atmospheric sciences* 37, 2712-2733, 1980.

351 Xu, B., Cao, J., Hansen, J., Yao, T., Joswia, D. R., Wang, N., Wu, G., Wang, M., Zhao, H., and  
352 Yang, W.: Black soot and the survival of Tibetan glaciers, *Proceedings of the National*  
353 *Academy of Sciences*, 106, 22114-22118, 2009a.

354 Xu, B., Wang, M., Joswiak, D. R., Cao, J. J., Yao, T. D., Wu, G. J., Yang, W., and Zhao, H. B.:  
355 Deposition of anthropogenic aerosols in a southeastern Tibetan glacier, *J. Geophys. Res.*, 114,  
356 D17209, 10.1029/2008JD011510, 2009b.

357 Xu, B., Cao, J., Joswiak, D. R., Liu, X., Zhao, H., and He, J.: Post-depositional enrichment of  
358 black soot in snow-pack and accelerated melting of Tibetan glaciers, *Environmental Research*  
359 *Letters*, 7, 014022, 2012.

360 Yao, T., Thompson, L., Yang, W., Yu, W., Gao, Y., Guo, X., Yang, X., Duan, K., Zhao, H., and  
361 Xu, B.: Different glacier status with atmospheric circulations in Tibetan Plateau and  
362 surroundings, *Nature Climate Change*, 2, 663-667, 2012.

363 Zhang, G., Kang, S., Fujita, K., Huintjes, E., Xu, J., Yamazaki, T., Haginoya, S., Wei, Y.,  
364 Scherer, D., and Schneider, C.: Energy and mass balance of Zhadang glacier surface, central  
365 Tibetan Plateau, *Journal of Glaciology*, 59, 137-148, 2013.

**Table 1.** Sampling information: Two expeditions were conducted on the Zhadang glacier, and samples (albedo, snow/ice) were collected under three melting conditions of the glacier in July and August of 2012. We measured the albedo five to six times at each site whilst collecting two to three snow/ice samples. In total, 120 albedo measurements and 48 snow/ice samples were obtained at the A - D sample sites in July, 2012 for the S-I and S-II conditions (Fig. 2). A total of 160 albedo samples and 64 snow samples were obtained at all sampling sites in August 2012. The albedo and concentrations of BC and dust are listed here.

Sample date	Sample site	Altitude (m a.s.l.)	Number of samples (albedo/snow & ice)	Average of albedo	Average of BC conc. (ppb)	Average of dust conc. (ppm)	Snow grain size (mm)	Snowpack density (kg/m <sup>3</sup> )	Snowpack Thickness (cm)	Solar zenith angle (°)	Cloud Amount (10=100%)	Scene type
July, 2012	A	5507	30/12	0.385	472.6	503.8	0.8 ~ 1.6	289 ~ 380	1	44.8~78.9	3~10	S-I
	B	5680	30/12	0.521	334.4	1891.9	0.6 ~ 1.6	289 ~ 350	1~2	52.3~75.8	1~10	
	C	5720	30/12	0.676	142.9	66.6	0.4 ~ 0.7	333 ~ 378	2~3	62.9~79.1	1~10	S-II
	D	5795	30/12	0.686	80.9	33.6	0.3 ~ 0.5	267~ 289	3	67.1~67.3	0~10	
August, 2012	A	5507	20/8	0.589	53.2	8.2	0.2 ~ 0.5	278 ~ 300	1~2	33.4~44	0~10	S-III
	B	5560	20/8	0.696	40.8	8.0	0.2 ~ 0.4	256 ~ 289	2~3	37.6~47.1	1~7	
	C	5626	20/8	0.710	55.5	7.0	0.2 ~ 0.4	267~ 311	2~3	40.8~50.2	0~7	
	D	5680	20/8	0.699	52.7	6.7	0.2 ~ 0.4	267~289	3	43.8~54.1	1~8	
	E	5695	20/8	0.708	55.2	6.4	0.2 ~ 0.4	267~289	3~4	45.8~57.9	0~6	
	F	5715	20/8	0.667	57.7	6.2	0.2 ~ 0.4	278~289	4	49.9~61.4	0~7	
	G	5750	20/8	0.698	59.4	5.2	0.2 ~ 0.3	222~244	5	51.9~64.6	0~7	
	H	5795	20/8	0.724	40.9	3.4	0.2 ~ 0.3	211~222	5	61.2~68.4	0~10	

**Table 2.** Sensitivity analysis with the SNICAR model. BC% and dust% are the contributions of BC and dust to the total reduction of the albedo, respectively.  $R_{in-short}$  is the incident solar radiation measured by AWS.

Date	Site	OA*	SA** pure	SA +BC	SA +BC & dust	BC%	dust%	$R_{in-short}$	RF +BC	RF +dust	Scene type
15 July	A	0.385	0.406	0.395	0.388	52	33	780.1	8.6	5.5	S-I
16 July	A	0.387	0.413	0.405	0.396	31	34	412.6	3.3	3.7	
15 July	B	0.363	0.406	0.394	0.364	28	70	548.2	6.6	16.4	
16 July	B	0.558	0.577	0.576	0.560	4	85	535.3	0.4	8.6	
14 July	C	0.618	0.640	0.631	0.624	41	32	1308.5	11.8	9.2	S-II
15 July	C	0.723	0.758	0.742	0.727	46	43	543.7	8.7	8.2	
16 July	C	0.745	0.756	0.754	0.752	18	18	604.4	1.2	1.2	
14 July	D	0.745	0.771	0.760	0.753	42	27	552.7	6.1	3.9	
15 July	D	0.732	0.754	0.745	0.740	41	23	648.4	5.8	3.2	
16 July	D	0.755	0.775	0.770	0.764	25	30	789.8	3.9	4.7	
24 Aug	A	0.568	0.791	0.786	0.784	2	1	337.8	1.4	0.7	S-III
25 Aug	A	0.653	0.682	0.681	0.680	5	2	658.7	0.9	0.5	
26 Aug	A	0.716	0.746	0.739	0.737	23	7	702.5	4.9	1.4	
24 Aug	B	0.759	0.793	0.779	0.778	41	4	608.1	8.5	0.9	
25 Aug	B	0.696	0.731	0.728	0.727	8	4	722.7	1.9	0.9	
26 Aug	B	0.656	0.683	0.681	0.68	7	4	736.2	1.5	0.7	
26 Aug	C	0.697	0.734	0.732	0.732	5	1	776.8	1.6	0.3	
24 Aug	D	0.726	0.806	0.797	0.795	11	3	822.6	7.4	1.6	
25 Aug	D	0.768	0.781	0.780	0.778	17	10	814	1.8	1.1	
26 Aug	D	0.647	0.781	0.779	0.778	1	1	811	1.3	1.0	
24 Aug	E	0.699	0.810	0.803	0.802	6	1	962	6.7	1.0	
25 Aug	E	0.780	0.813	0.809	0.807	12	6	891.5	3.6	1.8	
26 Aug	E	0.774	0.811	0.805	0.804	16	3	831	5.0	1.0	
24 Aug	F	0.792	0.839	0.835	0.833	9	4	786.8	3.1	1.6	
25 Aug	F	0.790	0.819	0.816	0.815	10	3	1030	3.1	1.0	
26 Aug	F	0.566	0.816	0.809	0.808	3	1	895	6.0	1.2	
24 Aug	G	0.795	0.848	0.840	0.838	15	4	1303	10.4	2.6	
25 Aug	G	0.806	0.828	0.824	0.823	18	5	1168	4.7	1.2	
26 Aug	G	0.652	0.819	0.812	0.811	4	1	932	6.5	0.9	
24 Aug	H	0.811	0.853	0.846	0.846	16	1	1134	7.5	0.6	
25 Aug	H	0.809	0.834	0.831	0.830	12	4	1316	3.9	1.3	
26 Aug	H	0.711	0.827	0.825	0.824	2	1	1192	2.4	1.2	
Avg.	S-I,II,III	0.684	0.741	0.735	0.731	18	15	826.1	4.7	2.8	

\* OA denotes observed albedo. \*\* SA denotes simulated albedo.



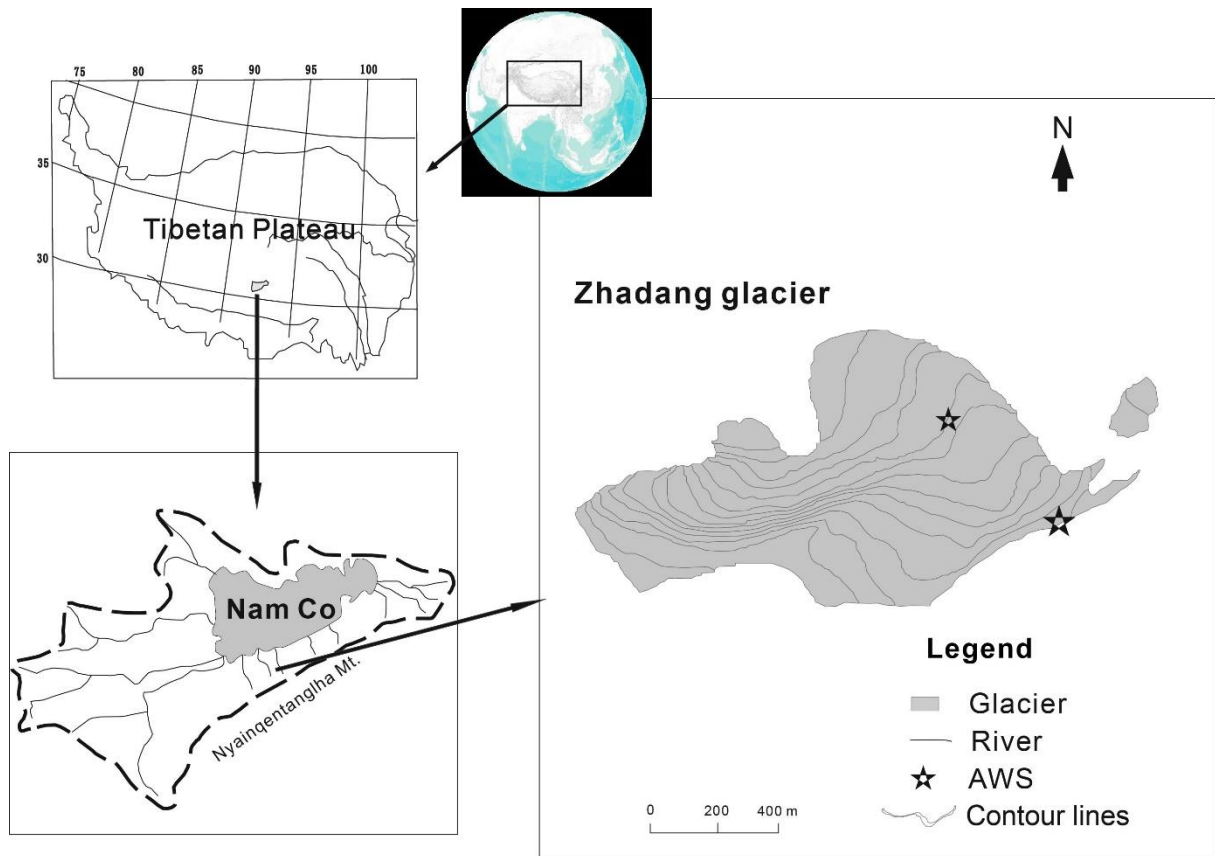


**Fig. 1.** Location of the Zhadang glacier on Mt. Nyainqentanglha.

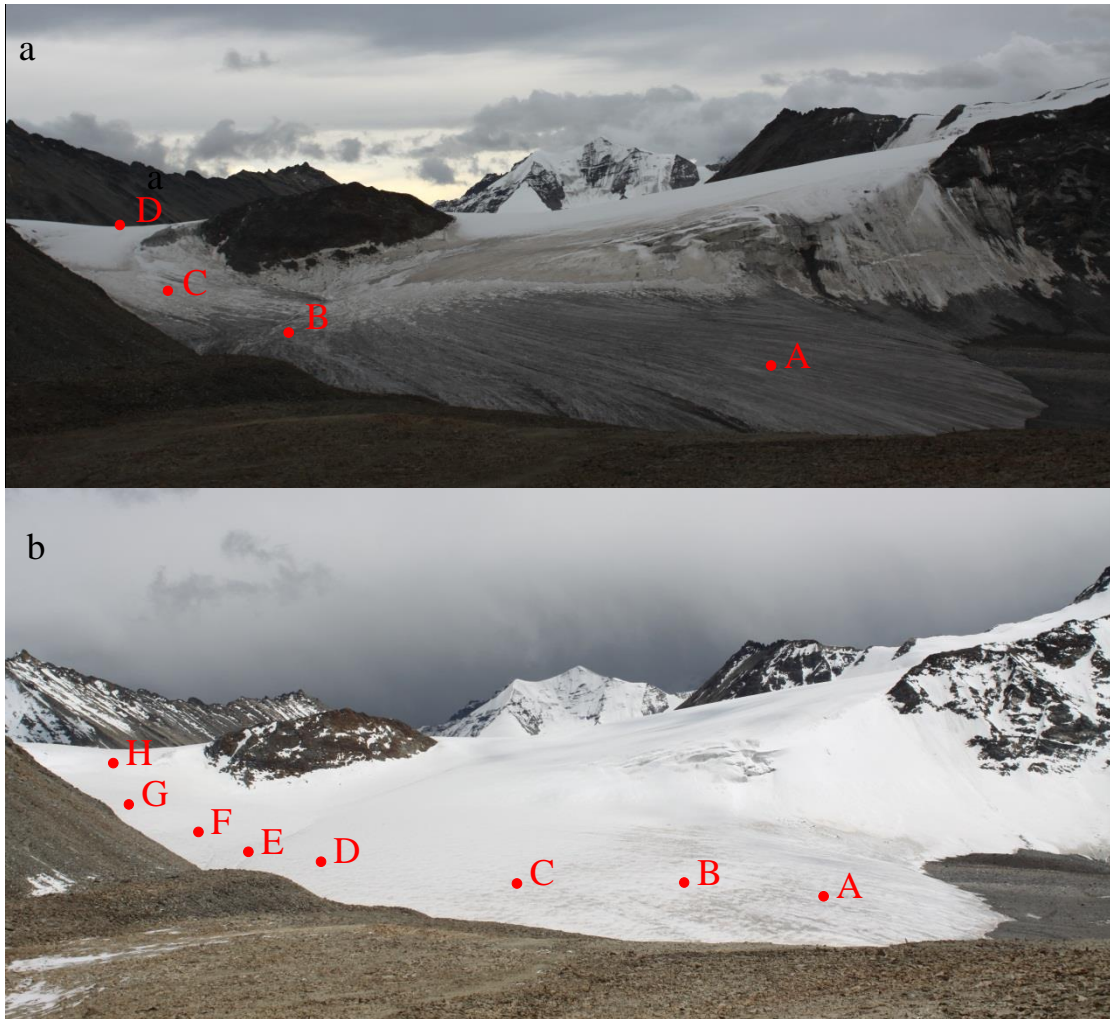


**Fig. 2.** Surface features of the Zhadang glacier on 16<sup>th</sup> Jul. (a) and 26<sup>th</sup> Aug. (b). The two surface conditions include three types of melting conditions: S-I: Sites A and B, which are located in the superimposed ice belt (Fig. 2a); S-II: Sites C and D, which are in the upper area of the glacier (Fig. 2a); S-III: All sites were covered by fresh snow (Fig. 2b).

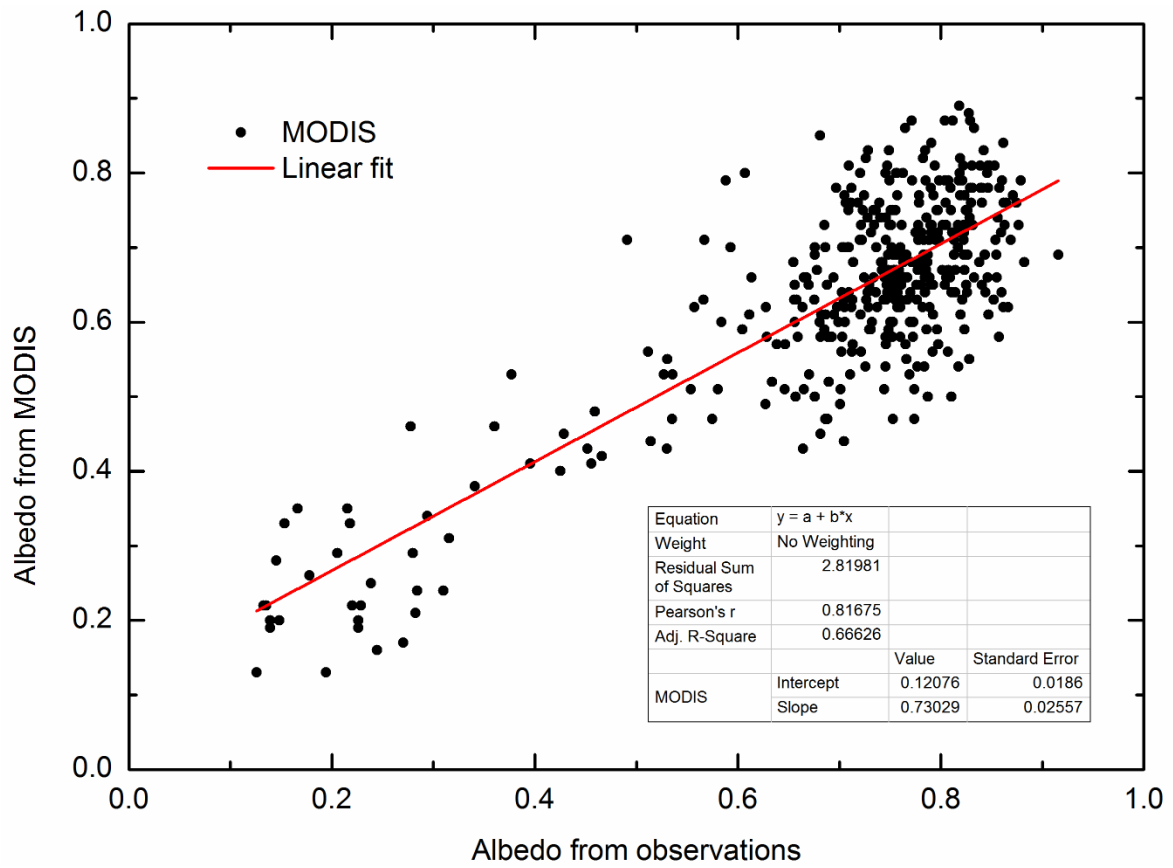


**Fig. 3.** The albedo of the pixel including the AWS in Zhadang glacier derived from MODIS and that observed by AWS in 2011.

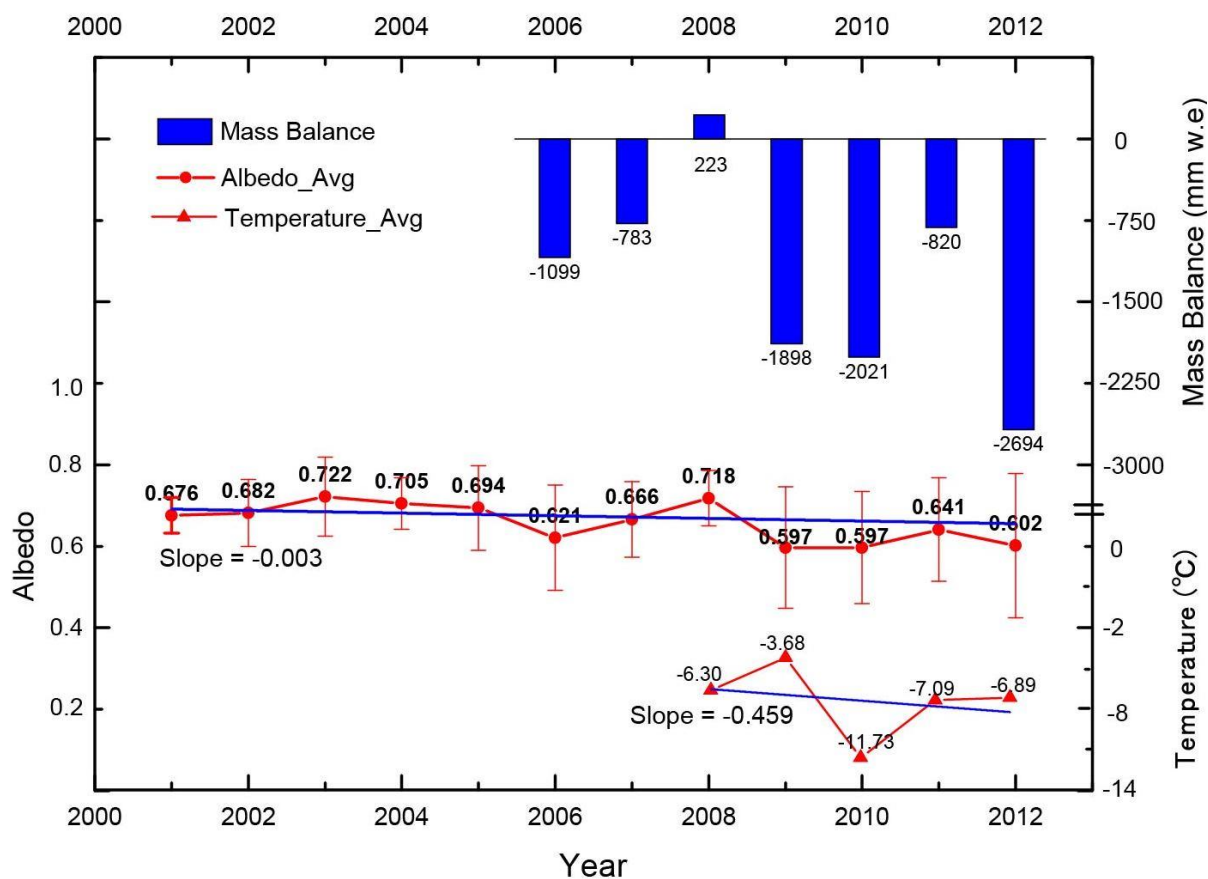


**Fig. 4.** Temporal changes of the albedo in the Zhadang glacier from 2000 to 2012 and the mass balance from 2006 to 2012. The albedo of the Zhadang glacier showed an overall downward trend in the last decade. Air temperature recorded by an AWS in the Zhadang glacier shows a slight decreasing trend.

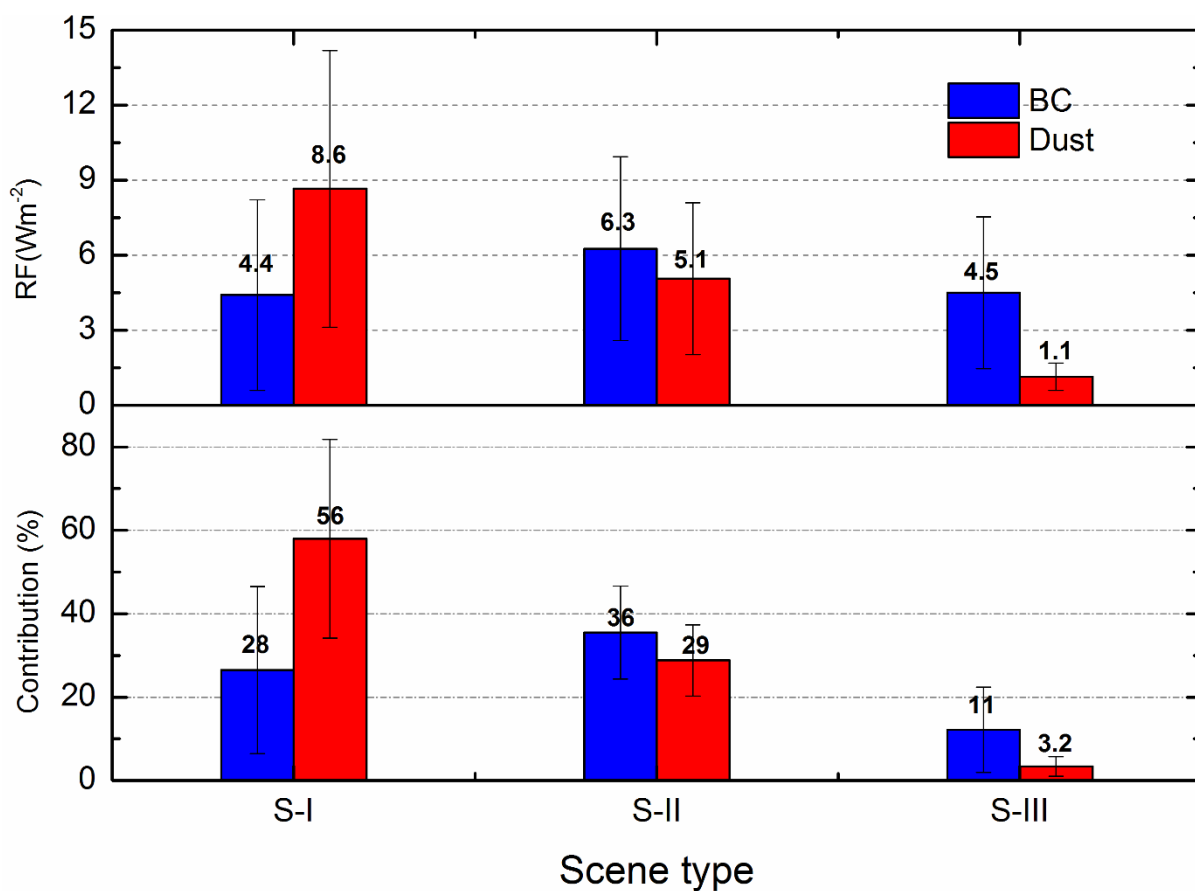


**Fig. 5.** Mid-day RFs of BC and dust on the Zhadang glacier and the contribution (results from the SNICAR model) show the reduction of the albedo in the surface snow cover area under three different melting conditions: S-I, where the surface of the glacier is bare ice; S-II, where the glacier is covered by aged snow; S-III, where the glacier is covered by fresh snow.

## Appendix

### Parameters for sensitivity analysis with SNICAR

1. Incident radiation (a. Direct, b. Diffuse); 2. Solar zenith angle; 3. Surface spectral distribution (a. Mid-latitude winter, clear-sky, cloud amount < 5. b. Mid-latitude winter, cloudy, cloud amount  $\geq 5$ ); 4. Snow grain effective radius ( $\mu\text{m}$ ); 5. Snowpack thickness (m); 6. Snowpack density ( $\text{kg}/\text{m}^3$ ); 7. Albedo of underlying ground (a. Visible, 0.3–0.7  $\mu\text{m}$ . b. Near-infrared, 0.7–5.0  $\mu\text{m}$ ); 8. MAC scaling factor (experimental) for BC; 9. Black carbon concentration (ppb, Sulphate-coated); 10. Dust concentration (ppm, 5.0–10.0  $\mu\text{m}$  diameter); 11. Volcanic ash concentration (ppm); 12. Experimental particle 1 concentration (ppb)

Date	site	1	2	3	4	5	6	7a	7b	8	9	10	11	12
14, July	C	b	79.1	b	600	0.02	378	0.15	0.3	11	129.9	56.4	0	0
14, July	D	b	67.3	b	400	0.05	289	0.15	0.3	11	77.2	29.6	0	0
15, July	A	b	78.9	b	800	0.01	289	0.13	0.12	11	608.2	649.3	0	0
15, July	B	b	75.8	b	800	0.01	289	0.13	0.12	11	657.3	3628.8	0	0
15, July	C	a	71.6	a	400	0.02	367	0.15	0.3	11	278	135.1	0	0
15, July	D	a	67.2	a	400	0.03	278	0.15	0.3	11	114	39	0	0
16, July	A	a	44.8	a	700	0.01	380	0.13	0.12	11	337	358.3	0	0
16, July	B	a	52.3	a	700	0.02	350	0.15	0.3	11	11.5	155	0	0
16, July	C	a	62.9	b	400	0.03	333	0.15	0.3	11	20.8	8.3	0	0
16, July	D	a	67.1	a	400	0.04	267	0.15	0.3	11	51.5	32.2	0	0
24, Aug	A	b	44	b	250	0.03	300	0.13	0.12	11	60.2	9.6	0	0
24, Aug	B	a	47.1	b	200	0.03	289	0.13	0.12	11	153.6	8.2	0	0
24, Aug	C	a	50.2	b	200	0.02	311	0.13	0.12	11	111.4	9	0	0
24, Aug	D	a	54.1	a	200	0.03	289	0.13	0.12	11	115.4	8.1	0	0
24, Aug	E	a	57.9	a	200	0.03	267	0.15	0.3	11	87.6	7.7	0	0
24, Aug	F	a	61.4	a	200	0.04	289	0.15	0.3	11	41.3	9.1	0	0
24, Aug	G	a	64.6	b	200	0.05	244	0.15	0.3	11	84.7	7.1	0	0
24, Aug	H	a	68.4	b	200	0.05	222	0.15	0.3	11	67.9	2.6	0	0
25, Aug	A	a	33.4	a	250	0.02	278	0.13	0.12	11	29.2	5.9	0	0
25, Aug	B	a	37.6	a	200	0.02	278	0.13	0.12	11	43.2	9.1	0	0
25, Aug	C	a	40.8	b	200	0.03	311	0.13	0.12	11	32.2	6.1	0	0
25, Aug	D	a	43.9	b	200	0.03	267	0.13	0.12	11	22.5	6.8	0	0
25, Aug	E	a	47	b	200	0.04	289	0.15	0.3	11	31.4	6.3	0	0
25, Aug	F	a	52	b	200	0.04	278	0.15	0.3	11	28.3	4.1	0	0
25, Aug	G	a	54	b	200	0.05	244	0.15	0.3	11	33.4	3.2	0	0
25, Aug	H	a	61.2	b	200	0.05	211	0.15	0.3	11	33.6	5.6	0	0
26, Aug	A	a	37.5	b	250	0.03	289	0.13	0.12	11	70.2	9.2	0	0
26, Aug	B	a	39.6	a	250	0.02	256	0.13	0.12	11	38.3	6.8	0	0
26, Aug	C	a	41.7	b	200	0.02	267	0.13	0.12	11	23	5.9	0	0
26, Aug	D	a	43.8	a	200	0.03	267	0.13	0.12	11	20.3	5.2	0	0
26, Aug	E	a	45.8	b	200	0.04	289	0.15	0.3	11	46.6	5.2	0	0

26, Aug	F	a	49.9	b	200	0.04	278	0.15	0.3	11	57.7	5.5	0	0
26, Aug	G	a	51.9	b	200	0.05	222	0.15	0.3	11	60	5.4	0	0
26, Aug	H	b	62.6	b	200	0.05	211	0.15	0.3	11	21.1	2.1	0	0

---

SNICAR online, <http://snow.engin.umich.edu/>